

# Re-utilization of germinal centers in multiple Peyer's patches results in highly synchronized, oligoclonal, and affinity-matured gut IgA responses

P Bergqvist<sup>1</sup>, A Stensson<sup>1</sup>, L Hazanov<sup>2</sup>, A Holmberg<sup>1</sup>, J Mattsson<sup>1</sup>, R Mehr<sup>2</sup>, M Bemark<sup>1,3</sup> and NY Lycke<sup>1,3</sup>

Whereas gut IgA responses to the microbiota may be multi-centered and diverse, little is known about IgA responses to T-cell-dependent antigens following oral immunizations. Using a novel approach, gut IgA responses to oral hapten (4-hydroxy-3-nitrophenyl)acetyl-cholera toxin (NP-CT) conjugates were followed at the cellular and molecular level. Surprisingly, these responses were highly synchronized, strongly oligoclonal, and dominated by affinity matured cells. Extensive lineage trees revealed clonal relationships between NP-specific IgA cells in gut inductive and effector sites, suggesting expansion of the same B-cell clone in multiple Peyer's patches (PPs). Adoptive transfer experiments showed that this was achieved through re-utilization of already existing germinal centers (GCs) in multiple PPs by previously activated GC GL7<sup>+</sup> B cells, provided oral NP-CT was given before cell transfer. Taken together, these results explain why repeated oral immunizations are mandatory for an effective oral vaccine.

## INTRODUCTION

Despite its central role, IgA antibody formation in the gut immune system is still incompletely understood.<sup>1</sup> In humans, several grams of IgA are produced each day, and this together with mucins and other soluble components constitutes the first line of defense of the gut mucosal barrier.<sup>2</sup> Plasma cells, at the effector site in the mucosal membrane, form IgA dimers, which are actively transported through the epithelium into the gut lumen as secretory IgA.<sup>3</sup> New IgA plasma cells are constantly generated in the gut through class switch recombination (CSR) of antigen-activated naïve IgM B cells, a process that has been found to depend greatly on the gut microbiota.<sup>4–7</sup> Most IgA CSR in the gut occur in the gut-associated lymphoid tissues (GALTs), which consist of Peyer's patches (PPs) and isolated lymphoid follicles (ILFs).<sup>8</sup> In addition, mesenteric lymph nodes (MLNs) and colon patches (cPs) have been ascribed an inductive role for mucosal IgA responses, the latter only following intrarectal immunizations.<sup>9</sup> An alternative, but quite controversial, site for IgA CSR is the non-organized lamina propria (LP) of the intestine.<sup>6,10–12</sup> Two main developmental pathways have been described for the generation of IgA plasma cells in

the gut LP: a T-cell-dependent (TD) and a T-cell-independent (TI) pathway.<sup>5,13</sup> In recent years, much interest has focused on the latter.<sup>5,6,12</sup>

The main site for IgA CSR in the mouse GALT is the PP.<sup>13–15</sup> This is true also for IgA responses against TI antigens, as we recently reported using CD40-deficient mice, which do not respond to TD antigens.<sup>16</sup> In addition, and in agreement with other studies, ILFs were also found to initiate IgA responses to TI antigens.<sup>12,17</sup> CD40-deficient mice had very little IgA CSR activity in the MLN and there was no evidence of IgA CSR in the LP of either the small intestine or the large intestine. We found that IgA CSR occurred in the PP in GL7-intermediate B cells in the complete absence of germinal centers (GCs). By contrast, in normal mice the PP constantly host GCs, which also allows for strong somatic hypermutation (SHM) in differentiating B cells.<sup>16,17</sup> The importance of PP GC and SHM of the gut IgA B-cell response for maintaining intestinal homeostasis with the bacterial microflora was recently elegantly shown by Wei *et al.*<sup>18</sup> Notably, contrary to peripheral lymph nodes and the spleen, GC formations are abundant in the PP even without immunization.<sup>19</sup>

<sup>1</sup>Mucosal Immunobiology and Vaccine Research Center (MIVAC), Department of Microbiology and Immunology, Institute of Biomedicine, University of Gothenburg, Gothenburg, Sweden. <sup>2</sup>The Mina & Everard Goodman Faculty of Life Sciences, Bar-Ilan University, Ramat-Gan, Israel. <sup>3</sup>Shared senior authors. Correspondence: NY Lycke (nils.lycke@microbio.gu.se)

Received 14 February 2012; accepted 3 May 2012; published online 11 July 2012. doi:10.1038/ml.2012.56

Much less detailed information is available on gut IgA B-cell responses to TD antigens, despite the vast literature on oral immunization and IgA responses in different mucosal tissues.<sup>6</sup> In particular, we lack an understanding of how the inductive process is organized so that an effective protective IgA immune response can be developed in the gut. More specifically, we still do not know how gut B cells are selected and expanded in response to an oral immunization and whether these cells undergo affinity maturation before seeding the LP of the mucosal membranes.<sup>1–4</sup> The inductive site for such responses has classically been ascribed to the PP, although the function of the MLN in this regard has not been investigated satisfactorily.<sup>14,20</sup> Several publications associate the MLN with IgA B-cell responses, as antigen can be transported by dendritic cells from the intestinal lumen to the MLN.<sup>20–22</sup> Especially, in colonizing germ-free mice with bacterial flora, the MLN has been found to be a site for IgA B-cell development.<sup>21</sup> Furthermore, the mouse intestine harbors a large number of ILFs hosting naïve B cells, which could potentially be activated by antigen and undergo IgA CSR.<sup>23,24</sup> This has been documented by several groups, but IgA CSR in the ILF has mostly, if not exclusively, been associated with TI antigens provided by the commensal flora.<sup>8</sup>

This study was designed to address the question of how TD IgA B-cell responses develop after oral immunization. To this end, we followed the buildup of a gut mucosal IgA response to the well-characterized hapten (4-hydroxy-3-nitrophenyl)acetyl (NP) conjugated to cholera toxin (CT), the most potent oral TD immunogen and adjuvant known today.<sup>25–27</sup> Despite numerous reports, we still lack information about how anti-CT IgA and IgG responses in the PP, MLN, LP, and spleen are connected and related.<sup>15,26–28</sup> Systemic IgG responses against NP have been extensively studied and it is well documented that such responses use a canonical rearrangement of the  $V_H186.2$  heavy chain to *DFL16.1* combined with  $\lambda 1$  light chains.<sup>29–31</sup> In addition, a single point mutation in  $V_H186.2$  that changes a tryptophan to a leucine at position 33 of the CDR1 region of the  $V_H$  gene increases the antibody affinity by at least 10-fold.<sup>29</sup> We have, thus, sequenced  $V_H186.2$  heavy-chain genes and investigated their isotype and SHMs. We found IgA responses to be highly synchronized, oligoclonal, and affinity matured, and broadly distributed to the inductive sites as well as to effector sites along the entire small and large intestines.

## RESULTS

### Repeated oral immunizations are required for intestinal IgA responses

To better understand how specific IgA antibody responses develop after oral immunization, we have explored the immune response to the well-characterized hapten NP conjugated to CT. Initial quality control tests of the conjugate confirmed that an optimal ratio of 7:1 of NP to CT did not affect the ability of CT to bind to the GM1-ganglioside receptor and reduced the *in vitro* ADP-ribosylating ability of CT by < 50% (**Supplementary Figure S1** online). Following one, two, or three NP-CT oral immunizations, we analyzed the specific IgA responses in the serum and small intestine. Whereas a single immunization gave

no or only poorly detectable NP-specific IgA responses in the serum and gut, two or three oral immunizations stimulated significant responses in both (**Figure 1a, b**). The frequency of NP- and CT-specific antibody-forming cells (AFCs) in the gut LP also increased with repeated oral immunizations (**Figure 1c**). NP-specific IgA response kinetics mimicked those against CT (**Figure 1a–c**), indicating that anti-NP IgA was a reliable marker for studies of oral immunogenicity of the holotoxin. It is worth noting that the number of oral immunizations rather than the time between doses appeared critical for the magnitude of the gut LP IgA AFC response (data not shown). The majority of anti-NP IgA AFCs were located in the proximal part of the small intestine (**Figure 1d**). This simply reflected the overall distribution of the total IgA plasma cells in the gut, as the frequency of NP-specific IgA AFCs was around 15% compared to all IgA AFCs in all compartments (**Figure 1d**).

### Specific IgA plasma cells appear along the entire small and large intestines following repeated oral immunizations

The NP-CT conjugate allowed us to follow the buildup of a specific IgA plasma cell response using antigen labeling of plasma cells in frozen sections of the small and large intestines, which is normally difficult with CT alone because of the abundance of GM1-ganglioside receptors that bind CT in the gut.<sup>32</sup> Whereas no or only few NP-specific IgA plasma cells were found after a single immunization, three oral immunizations with NP-CT stimulated the formation of high anti-NP IgA plasma cell numbers along the entire small and large intestines (**Figure 2**). Notably, no clusters of NP-specific cells were observed, suggesting that the B cells emanated from a distal source and seeded the LP, rather than expanded locally in the ILF or *in situ* in the LP (**Figure 2a–c**). The distribution of NP-specific plasma cells reflected the overall distribution of the total IgA plasma cells, even within a single villus (**Figure 2d**). It is worth mentioning that at no time were NP-specific plasma cells observed in the inductive sites of the GALT, i.e., the PPs, cPs, or ILFs, and only occasionally in the MLNs (not shown), suggesting that the potential inductive sites in the GALT largely lacked specific IgA plasma cells following oral immunizations (**Figure 2e–h**). Thus, IgA plasma cells were present in the LP along the entire small and large intestines and did not show any local expansion in the ILF or the non-organized LP of the gut mucosa.

### TD gut IgA B-cell responses are strongly selected for high-affinity maturation

A classical polymerase chain reaction (PCR) method was used to analyze NP-specific  $V_H$  gene transcripts of different isotypes in gut inductive and effector tissues.<sup>29–31,33</sup> We amplified  $V_H186.2$ -IgM or  $V_H186.2$ -IgA transcripts from cDNA prepared from MLNs, PPs, and small or large intestines of mice orally immunized one or three times with NP-CT, and analyzed them for the presence of  $V_H186.2$ -*DFL16.1* rearrangements by Southern blotting (**Figure 3a,b**). We detected low levels of NP-specific IgM transcripts in the PP after a single oral immunization with NP-CT, while other tissues, including the MLN, hosted few or no NP-specific IgM transcripts (**Figure 3c** and data not shown).

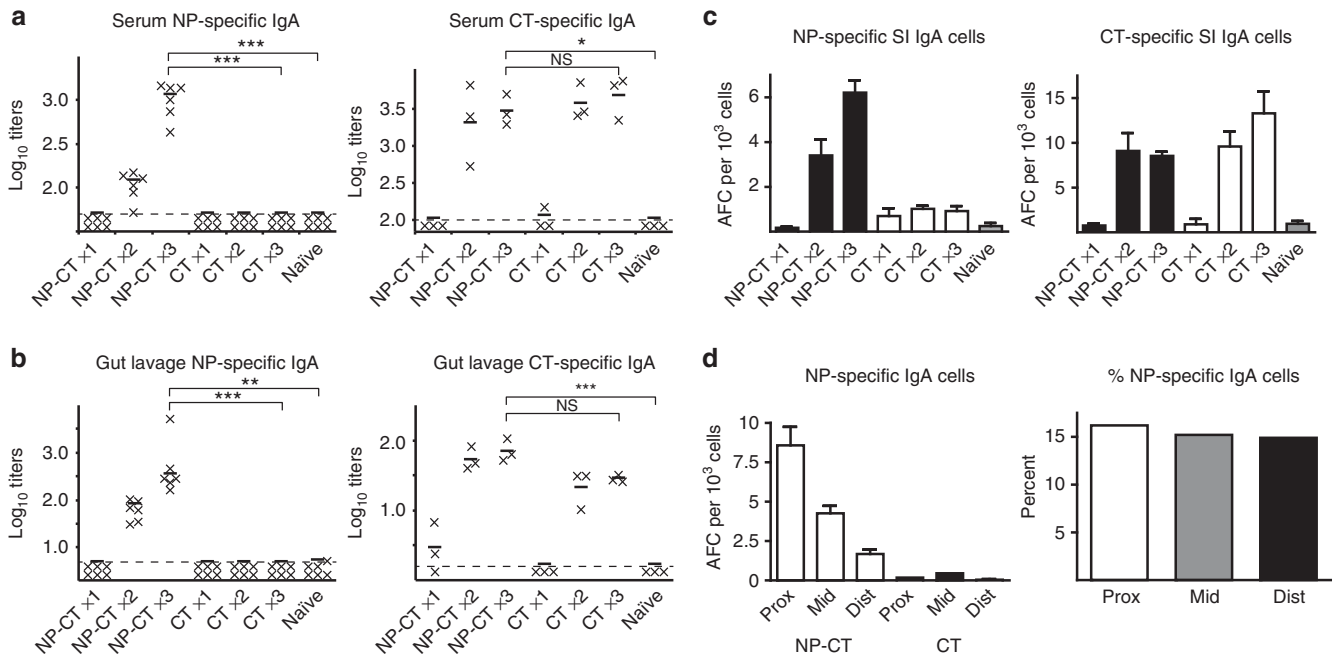


**Figure 1** Repeated oral immunizations are required for stimulation of antigen-specific serum and gut IgA responses. Mice in groups of three were orally immunized one, two, or three times with hapten (4-hydroxy-3-nitrophenyl)acetyl-cholera toxin (NP-CT) or CT alone. The log<sub>10</sub> titers of NP- and CT-specific IgA antibodies in (a) the serum and (b) gut lavages from individual mice are shown. (c) Plasma cells were isolated from the small intestine (SI) by repeated digestions with collagenase of small pieces of tissue as described previously<sup>52</sup> and the number of NP- and CT-specific antibody-producing cells (AFCs) were determined. Values are given as mean AFC value per 10<sup>3</sup> cells ± s.d. (d) The SIs were divided into proximal (Prox), middle (Mid), and distal (Dist) sections, and the anti-NP IgA AFC activity was determined following three oral immunizations with NP-CT or CT (left panel) and the frequency of specific anti-NP IgA AFC per total IgA AFC was calculated (right). (a–d) All data are representative results of two experiments giving similar results. The levels of NP-specific antibodies in serum and gut lavages were determined simultaneously for both experiments and pooled data are shown, whereas levels of CT were independently determined and data derived from one of the experiments are shown. Kruskal–Wallis analysis showed that the distribution was non-random ( $P < 0.001$  for (a) and (b, right),  $P = 0.004$  for (b, left)), and Dunn's post-test showed that there were significant differences between columns as indicated (NS:  $P \geq 0.05$ , \* $P < 0.05$ , \*\* $P < 0.01$ , \*\*\* $P < 0.001$ ). Details about the NP-CT conjugate can be found in **Supplementary Figure S1** online.

The level of NP-specific IgM transcripts in the PP was not significantly increased after three oral immunizations, suggesting that the majority of B cells underwent IgA CSR in the PP following oral immunizations (Figure 3c). This was confirmed by the predominant expression of IgA-switched *V<sub>H</sub>186.2-DFL16.1* CDR3 transcripts in the PP and MLN, as well as in both the small and large intestines after three as opposed to a single oral immunization (Figure 3d). Hence, strong IgA NP-specific *V<sub>H</sub>186.2-DFL16.1* CDR3 gene expression required multiple oral immunizations. Of note, before these experiments, we confirmed that our PCR method detected *V<sub>H</sub>186.2-IgA* transcripts from both B cells and plasma cells<sup>34,35</sup> (Supplementary Figure S2 online). Moreover, only few *V<sub>H</sub>186.2-IgM* transcripts could be detected at any time in the GALT, suggesting that most B cells undergo IgA CSR early during the response. Furthermore, the kinetics and magnitude of *V<sub>H</sub>186.2-IgA* transcript expression in the different tissues suggested an inductive process emanating from the PP.

To analyze whether NP-specific B cells and plasma cells isolated from the different tissues after oral immunizations were clonally related and had undergone affinity maturation, *V<sub>H</sub>186.2-IgA* transcripts from the MLN, PP, or small and large intestines were cloned. A majority of clones that hybridized to our NP probe indeed contained canonical NP-binding

transcripts, while such sequences were not present in bacterial clones that did not hybridize (Figure 4a). The level of mutations in unique NP-binding *V<sub>H</sub>186.2-DFL16.1* sequences increased after repeated oral immunizations (Figure 4a). For comparison, we found that the level of mutations in non-NP-binding sequences in the gut was similar to that of NP-binding sequences from orally immunized mice, demonstrating that gut NP-binding plasma cells were, indeed, subject to similar mutational activity as gut plasma cells in general (Figure 4a).

A single mutation in the CDR1 region,  $W_{33} \Rightarrow L_{33}$ , is known to increase the affinity of anti-NP antibody by at least 10-fold.<sup>29</sup> Therefore, we investigated whether this mutation was present in transcripts from any of the tissues. Following two oral immunizations, the affinity-increasing mutation had already appeared in the PPs and MLN, constituting a majority of specific transcripts (50–70%), whereas the LP still hosted relatively few (20%) high-affinity NP-specific IgA plasma cells (Figure 4b). In contrast, after three oral immunizations, roughly 60% of the sequences from the small intestine carried the high-affinity mutation, indicating a strong accumulation of high-affinity plasma cells after the third immunization (Figure 4b). A similar pattern was found for NP-binding sequences from IgA plasma cells in the colon (Figure 4b).

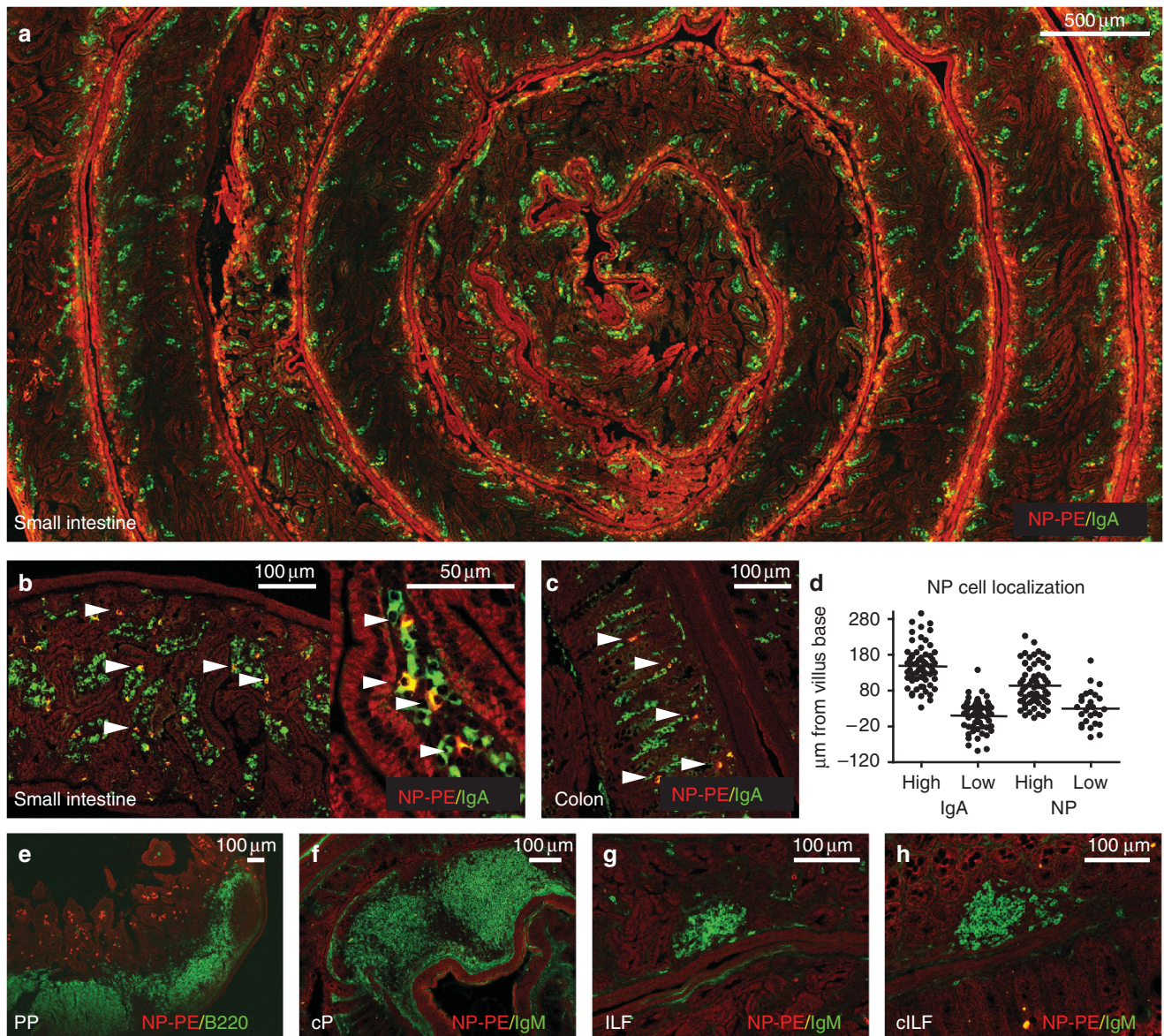


**Figure 2** Following oral immunizations hapten (4-hydroxy-3-nitrophenyl)acetyl (NP)-specific IgA<sup>+</sup> plasma cells are present in the lamina propria along the entire small and large intestine, but not in the gut-associated lymphoid tissue (GALT). Representative micrographs of GALT and the small and large intestines from three mice immunized three times with NP-cholera toxin (CT). (a) Swiss roll sections of small intestines were labeled with NP-PE (red) and anti-IgA FITC (green). (b and c) High-magnification close-ups of representative sections from the small intestine (b) and the colon (c) are shown, with arrows marking NP-specific IgA plasma cells (yellow). (d) The distribution of NP-specific and total IgA plasma cells in individual villi. We measured the distance between the base of the villi and the location of IgA plasma cells. We found that NP-specific IgA plasma cells distributed similarly to overall total IgA plasma cells in each individual villi. The dots represent the mean distance from the base of the villus and the bars indicate mean values for three mice in each group. (e–h) Representative micrographs of GALT showing lack of anti-NP IgA plasma cells following oral immunizations are shown. Sections from Peyer's patch (PP), colon patch (cP), small intestinal ILF (ILF), and colon ILF (cILF) are shown after labeling with NP-PE and anti-B220 FITC or anti-IgM FITC (green), as indicated. We defined cP on the basis of clusters of > 100 B220<sup>+</sup> cells in a section, which also contained cells labeling with anti-GL7 antibodies, whereas colon ILFs were < 100 cells and no cells labeling with anti-GL7 antibodies. These are representative results of three experiments giving similar results.

### A synchronized selection process in the PP allows for a highly oligoclonal IgA B-cell response in the entire gut immune system

Because very few NP-binding transcripts were identified after one oral immunization, we focused our further efforts on dissecting the distribution of  $V_H186.2$ -IgA genes sharing identical CDR3 regions in the different tissues of the gut immune

system after three oral immunizations. Sequence analysis in four individual mice revealed extensive clonality between NP-specific IgA-producing B cells and plasma cells recovered from the different tissues (Figure 5a). In fact, B cells that were part of the same clone were present at both inductive and effector tissues following oral immunization with NP-CT (Figure 5a). Moreover, a pattern of a highly oligoclonal NP-specific IgA

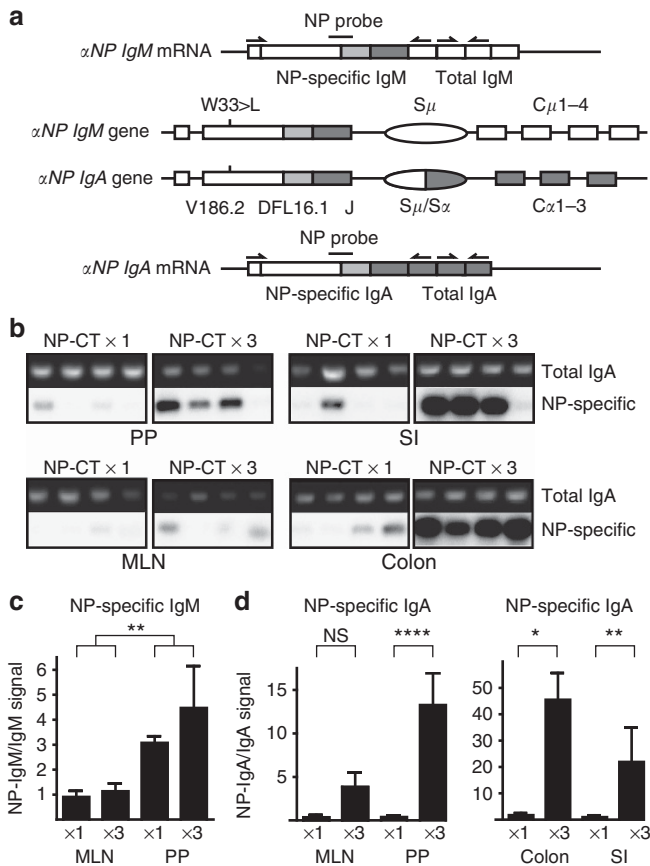


**Figure 3** Canonical hapten (4-hydroxy-3-nitrophenyl)acetyl (NP)-recognizing *V<sub>H</sub>186.2-DFL16.1* transcripts are enriched in the gut mucosal inductive as well as effector tissues following repeated oral immunizations. A specific *V<sub>H</sub>186.2-DFL16.1* gene recombination event dominates anti-NP B-cell responses. **(a)** Immunoglobulin heavy-chain transcripts were polymerase chain reaction (PCR) amplified using a *V<sub>H</sub>186.2* upstream primer together with IgM- or IgA-specific downstream primers, and were probed with a CDR3-specific probe specific for NP-recognizing *V<sub>H</sub>186.2-DFL16.1* recombination events after Southern blotting. As a control for expression of IgA and IgM, constant regions were amplified separately. **(b)** Examples of primary data from the analysis of *V<sub>H</sub>186.2-DFL16.1* gene expression in IgA cells present in the different tissues. The upper part of each panel shows PCR assays designed to determine the total amount of IgA in the sample (the constant region primer pairs in **a** stained with ethidium bromide) and the lower part Southern blot assays to determine expression of NP-binding heavy-chain transcripts (the variable/constant region primer pair in **a**, labeled with the NP probe after electrophoresis and transfer). **(c)** The relative expression of IgM transcripts carrying NP-specific CDR3 region were determined in the mesenteric lymph node (MLN) and Peyer's patch (PP) from mice orally immunized one or three times with NP-cholera toxin (CT). The difference between MLN and PP was significant (Mann–Whitney test,  $P=0.0039$ ). No significant expression of NP-specific IgM transcripts was detected in the small intestine (SI) or colon at either time point (data not shown). **(d)** The relative expression of IgA transcripts carrying NP-specific CDR3 regions was determined in MLN, PP, colon, or SI following one or three oral immunizations with NP-CT. These are representative results of three experiments giving similar results. Organs from nine mice were included in the test. The increased levels of IgA NP signals after one vs. three immunizations were significant as indicated (MLN, NS,  $P=0.0635$ ; PP, \*\*\*\* $P<0.0001$ ; colon, \* $P=0.0159$ ; and SI, \*\* $P=0.0051$ ).

responses was evident in all analyzed mice following oral immunization (**Figure 5b**). A majority of these clones had undergone affinity maturation showing the  $W_{33} \Rightarrow L_{33}$  mutation in the CDR1 region (**Figure 5b**). This was prominent in all mice and indicated that NP-binding IgA B cells were subject to a strong selection pressure in the GALT following oral immunizations. Notably, this selection process required multiple oral immunizations, as the level of mutations and affinity maturation was improved after three as opposed to two oral immunizations. Thus, repeated oral antigen exposure of the gut immune system was a driving force for selecting high-quality IgA plasma cells.

The clonality of the response raised the question of whether individual PPs hosted unique high-affinity IgA B-cell clones, or if one clone could be shared by many PPs, indicating migration of this B-cell clone into other PPs. Sequence analysis was performed of *V<sub>H</sub>186.2-IgA* genes from individual PPs. Remarkably, we found the same clones represented in multiple PPs, and several examples where the same NP-specific IgA B-cell clone was present in all four PPs analyzed from one mouse (**Figure 6a**). In addition, the response in the PP of individual mice was clearly oligoclonal and was always dominated by a limited number of clones. In general, individual mice hosted unique clones not found in other mice (**Figure 6b**). These results reflected a strong selection process favoring expansion of high-affinity NP-specific IgA B-cell clones in the GALT following oral immunization. Indeed, it appeared as if this was achieved through an early distribution of a few high-affinity IgA B-cell clones from one to multiple PPs following immunization, and that each subsequent immunization promoted the expansion of these selected clones in all PP.

Next, we wanted to exclude the possibility of contamination of plasma cells from the LP into the PP B-cell preparation. Therefore, we performed microdissection of individual PPs from frozen intestinal tissues. We also included cP in this analysis, as this organized lymphoid structure has been claimed to provide comparable functions to the PP, as an inductive site for colon LP responses.<sup>9</sup> Although cPs are not readily identified macroscopically, microdissection allowed us to analyze them separately from other gut tissues. Sequence analysis of NP-binding *V<sub>H</sub>186.2-IgA* genes from microdissected PP confirmed our previous observation that NP-binding IgA B-cell clones in the PP were, indeed, clonally related with plasma cells in the LP effector sites, and that the response was oligoclonal with some high-affinity clones dominating (**Figure 6c**). Interestingly, cP did in some cases host the same dominating NP-binding IgA B-cell clones as PP, suggesting that the cP exchanged cells with PP, and could be considered inductive sites in the GALT (**Figure 6c**).

**Extensive lineage trees reflect a highly synchronized system for the distribution of specific gut IgA B-cell responses**

Lineage tree analysis of *V<sub>H</sub>186.2-IgA* genes isolated from inductive and effector sites confirmed an extensive distribution and oligoclonal domination of NP-specific IgA B cells in the entire

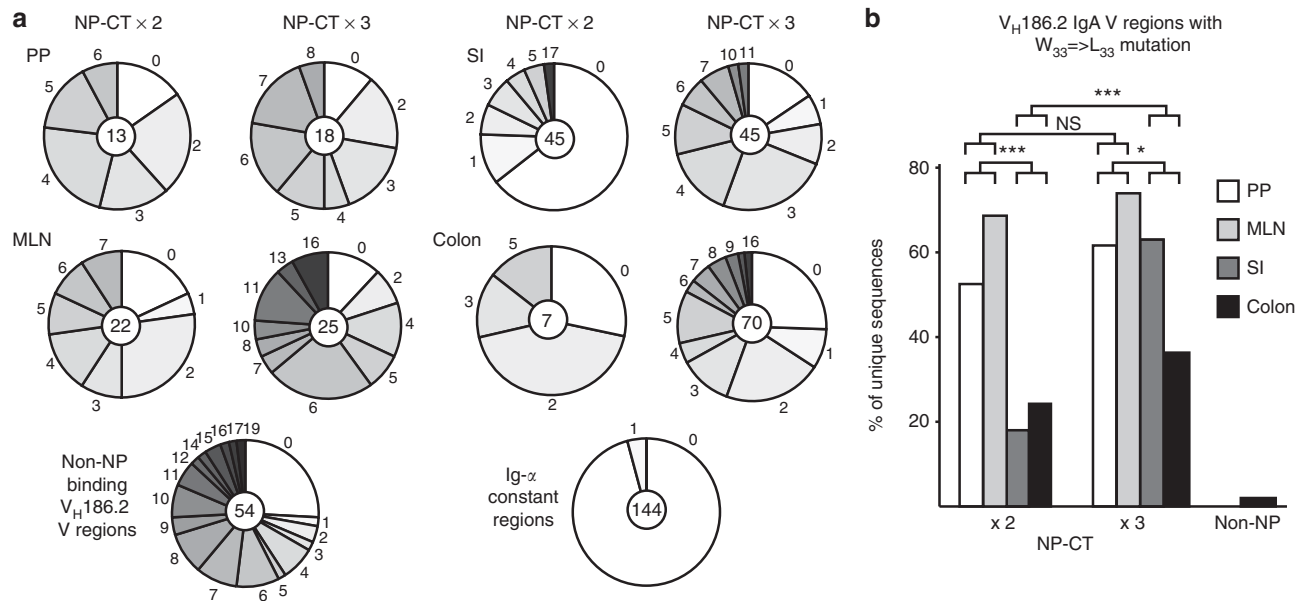


**Figure 4** Induction of high levels of antigen-specific IgA transcripts and affinity maturation in the gut immune system is dependent on repeated oral immunizations. **(a)** *V<sub>H</sub>186.2-IgA* gene transcripts were polymerase chain reaction (PCR) amplified and cloned. Potentially hapten (4-hydroxy-3-nitrophenyl)acetyl (NP)-binding sequences were identified using colony hybridization with a CDR3 probe, and were confirmed as NP-binding after sequencing (see Methods). The pie charts depict the frequency of unique clones containing different numbers of mutations in their V regions in Peyer's patches (PPs), mesenteric lymph nodes (MLNs), small intestine (SI), and colon after two or three oral immunizations with NP-cholera toxin (CT). Values are given for the number of mutations observed and the number of sequences analyzed (center of pie chart). Single pie charts in the lower panel depict the frequency of mutations in non-NP binding *V<sub>H</sub>186.2*-containing clones (left), and the mutation frequency in the constant IgA region that was co-amplified with the *V<sub>H</sub>186.2* V region (right). **(b)** The percentage of IgA sequences hosting the  $W_{33}=>L_{33}$  mutation in PP, MLN, SI, and colon after two (2x) and three (3x) oral immunizations as compared to that in non-NP-binding sequences with *V<sub>H</sub>186.2* recombined antibody heavy chains. These are representative results of two experiments giving similar results. In each experiment, cells from three mice were pooled. There were significant differences between inductive (PP, MLN) and effector (SI, colon) sites after two ( $P=0.003$ ) and three ( $P=0.0149$ ) oral immunizations, and between two and three oral immunizations at effector ( $P=0.001$ ) but not inductive ( $P=0.6288$ ) sites. Further data regarding induction of NP-specific transcripts can be found in **Figure 3**. NS, not significant.

gut immune system<sup>36</sup> (**Figure 7**). The trees of clonally related NP-specific IgA B cells were widely distributed in all tissues, i.e., several different PPs, the MLN, distal and proximal small intestine, and the colon (**Figure 7**). Hence, the clonality between specific NP-binding gut IgA B cells and plasma cells was not just along the axis of a single PP to MLN and the LP of the small intestine, but rather a widely distributed representation of the clone in all tissues following oral immunizations. The affinity-enhancing  $W_{33}=>L_{33}$  mutation was identified as an early event in most of these trees, followed by the introduction of additional mutations that were not shared between clones (**Figure 7**). This striking B-cell clonality clearly suggested that NP-specific IgA B cells were subjected to a strong selection process in the PP before seeding the LP of both the small and large intestines (**Figure 7**). Thus, it appeared that the IgA response to TD antigens was effectively synchronized from multiple PPs and then widely distributed throughout the entire gut mucosal immune system.

#### Adoptive transfer of NP-specific BCR transgenic B cells confirms a highly synchronized IgA B-cell expansion in multiple PPs

Finally, we capitalized on a high-affinity B1-8<sup>hi</sup> NP-specific IgH knock-in B-cell transfer model to visualize the expansion and

distribution of GFP<sup>+</sup> NP-specific B cells and plasma cells following oral immunization (**Figure 8a**). The largest expansion of GFP<sup>+</sup> NP-specific B cells was found in the PP as compared to the MLN or the spleen following oral NP-CT immunizations (**Figure 8b, c**). NP-specific GFP<sup>+</sup> B cells were found exclusively in the GL7<sup>+</sup> IgD<sup>-</sup> κ-chain population located in GCs of the PP, indicating an efficient activation of specific B cells present in the PP by oral immunization (**Figure 8b**). The frequency of GFP<sup>+</sup> NP-specific GL7<sup>+</sup> B cells in pooled PPs from individual mice increased only slightly (8–12%) after three oral immunizations as compared to that after a single dose (**Figure 8d**). However, individual PPs analyzed along the small intestine hosted few NP-specific B cells at distal sites, whereas proximal PPs were significantly more involved in the GFP<sup>+</sup> NP-specific B-cell response after a single dose. This pattern was lost after three oral immunizations, when distal and proximal PPs hosted comparable levels of GFP<sup>+</sup> NP-specific B cells, suggesting an effective distribution of activated GFP<sup>+</sup> B cells to multiple PPs after the first oral immunization (**Figure 8c**). Individual PPs accumulated GFP<sup>+</sup> NP-specific B cells in GCs. As opposed to the expansion of specific B cells in GCs in the MLN or the spleen after intraperitoneal immunizations with NP-CGG, these GFP<sup>+</sup> cells were less tightly clustered in GCs, likely reflecting expansion in preformed GCs rather than GCs formed *de novo* in the

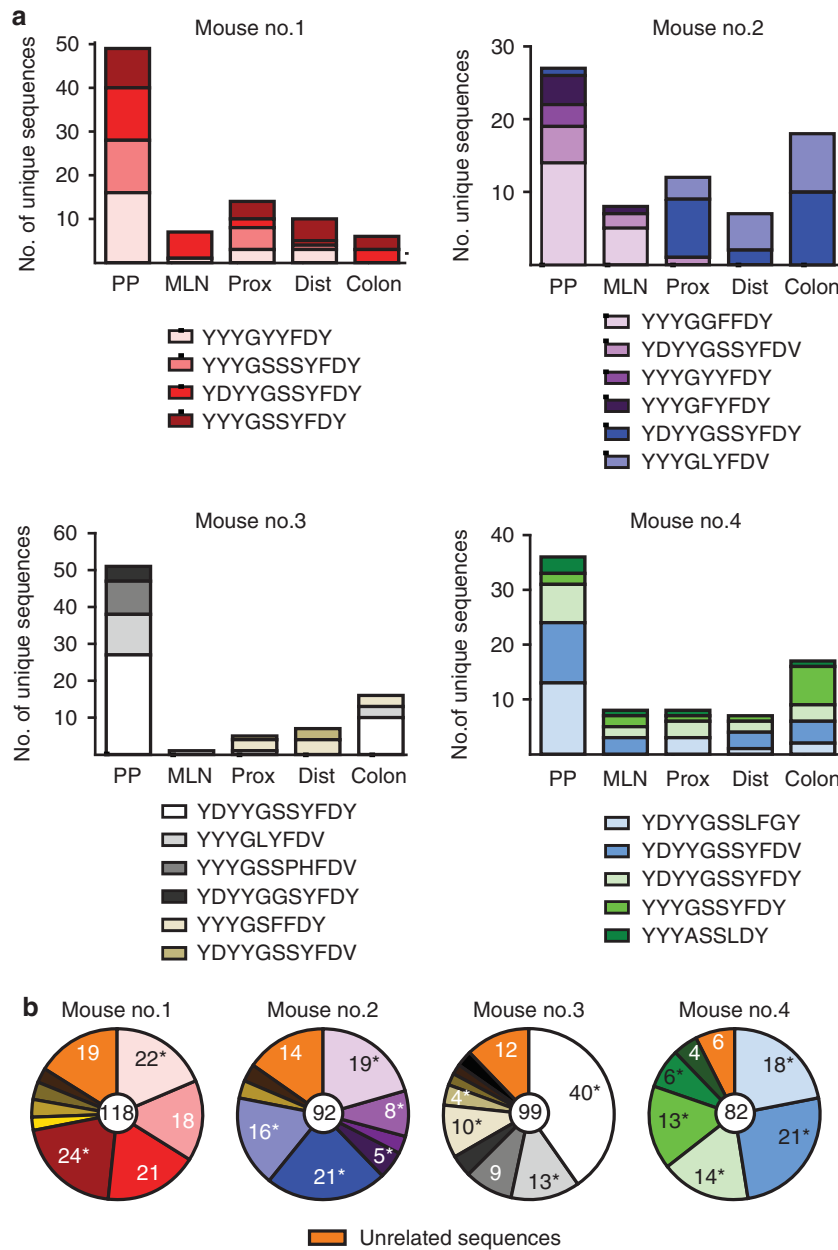


**Figure 5** Gut IgA responses are dominated by a small number of affinity-matured B-cell clones that are shared between inductive and effector sites. **(a)**  $V_H186.2$ -DFL16.1 IgA gene transcripts were isolated from Peyer's patches (PP), mesenteric lymph nodes (MLNs), proximal (Prox) and distal (Dist) small intestine, and colon from four mice that had been orally immunized three times with hapten (4-hydroxy-3-nitrophenyl)acetyl-cholera toxin (NP-CT). Sequences from different tissues in individual mice were analyzed for identical CDR3 regions based on their DNA sequence. The graphs depict the numbers of unique sequences for the dominating clones in each tissue. **(b)** All  $V_H186.2$ -DFL16.1 IgA gene transcripts isolated from different tissues in individual mice were pooled, and the relative contribution of different clones is indicated. The numbers in the sectors indicate the number of unique sequences within that clone and the number in the middle, the total number of unique sequences analyzed in each mouse. Stars indicate clones that host the  $W_{33} = >L_{33}$  high-affinity mutation. When sequences were compared within a single mouse, on average 87% (range 84–92% for the mice) of the 391 sequences belonged to a clone, which was significantly different from the 43% that could be assigned to a clone in any of the other mice ( $P > 0.0001$ ; Fisher's exact test).

PP (Figure 8e–g). Moreover, NP-specific GFP<sup>+</sup> IgA plasma cell frequencies were significantly higher in the small compared to the large intestine or the spleen after oral NP-CT immunizations (Figure 8i–k). Importantly, this model also confirmed our previous estimation that roughly 15% of the total IgA plasma cells in the small intestine were specific for NP following multiple

oral immunizations with NP-CT (Figure 8j). Considering that this is only one epitope in NP-CT, this observation is, indeed, remarkable.

To prove that cells already existing in one PP GC had the ability to achieve a highly synchronized gut IgA response following oral immunization through invasion of existing GC, we adoptively

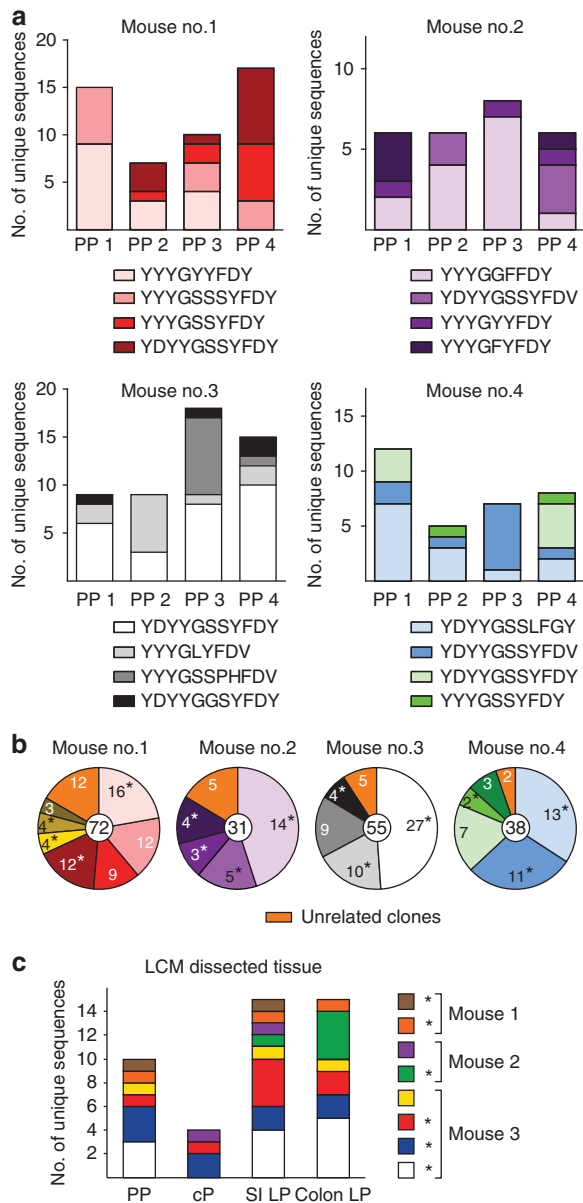


**Figure 6** Clonally related antigen-specific IgA sequences are shared between multiple Peyer's patches (PPs) following oral immunization. **(a and b)** Four mice were given three oral immunizations with NP-CT and  $V_H186.2$ -DFL16.1 IgA gene transcripts were isolated from four separate PPs in individual mice. The gene sequences were analyzed and compared to dissect whether the PP in individual mice hosted shared clones. When sequences were compared within a single mouse, on average 88% of the 196 sequences belonged to a clone, which was significantly different from the 44% that could be assigned to a clone in any of the other mice ( $P > 0.0001$ ; Fisher's exact test). **(c)** To control for that  $V_H186.2$ -DFL16.1 IgA gene transcripts in PPs were not confounded by transcripts derived from the lamina propria (LP) we undertook cryosectioning of the small (SI) and large intestines from three mice to better separate PP from LP using laser capture microscopy. We obtained materials from PP, colon patches (cPs) and LP from the SI and the colon. After preparation of RNA,  $V_H186.2$ -DFL16.1 NP-binding IgA gene sequences were isolated and analyzed. Out of 66 unique sequences, 44 shared CDR3 regions at distinct sites; the mice they were derived from and the number of unique sequences from each organ are indicated in the diagram. Stars indicate clones that host the  $W_{33} > L_{33}$  high-affinity mutation. LCM, laser capture microdissection.

transferred GL7<sup>+</sup> high-affinity B1-8<sup>hi</sup> NP-specific B cells from PP from mice given a single oral immunization with NP-CT to naïve recipient mice. Strikingly, we could only detect GFP<sup>+</sup> NP-specific B cells in multiple PPs in mice receiving an oral dose of NP-CT 24 h before transfer, while the PP in mice given no antigen or an oral-dose NP-CT at 24 h after the cell transfer failed to host any NP-specific GFP<sup>+</sup> B cells (**Figure 8l-n**). Whereas cells entering PP eventually lost their GC phenotype, suggesting proliferation and differentiation, cells in the MLN maintained a GC phenotype outside of the GC. Thus, GL7<sup>+</sup> PP B cells from orally primed mice can migrate into existing GC in multiple PPs, provided the antigen is present in the GC before transfer of the PP GL7<sup>+</sup> B cells. This experiment explains why repeated oral immunizations with TD antigens are critical for a synchronized and effective IgA response in the gut mucosa.

## DISCUSSION

In this study, we provide new insights into how gut mucosal IgA B-cell responses against TD antigens are established following oral immunizations. For the first time, we can report that gut IgA B-cell responses were found to be oligoclonal and had undergone extensive SHM in a process that was highly synchronized and set to strongly select for high-affinity B cells. This was achieved by the distribution of antigen-responding GC B cells from one PP to multiple PPs following priming, such that repeated exposures with the antigen selected and expanded the same B-cell clones in many, perhaps all, PPs in the inductive phase (**Figure 9**). Hence, subsequently antigen-selected, affinity-matured, B-cell clones dominated the response in the entire gut immune system, including the inductive sites in the GALT as well as the effector sites in the LP of the small and large intestines. Thus, the selection process was highly synchronized within the GALT to result in only a few original B-cell clones that later dominated and produced high-affinity antigen-specific IgA in the LP. This was achieved through re-utilization of already existing GC in multiple PPs as we could demonstrate with adoptive transfer experiments, in which GFP<sup>+</sup>GL7<sup>+</sup>PP B cells from orally immunized mice repopulated GCs in multiple PPs in recipient mice, provided oral antigen was given to the recipients before transfer. It is worth mentioning that the distribution of antigen-specific plasma cells in the gut was found to be proportional to the overall distribution of IgA plasma cells, clearly arguing in favor of a system seeding specific cells from a central inductive site in the GALT along the entire mucosal membrane.<sup>2,17,37,38</sup> No evidence of local induction or expansion of specific B-cell responses in the ILF or the gut LP was found. Furthermore, and in contrast to systemic antibody responses, IgM B cells were driven to undergo CSR to IgA in the GALT at an early stage of differentiation, leaving very few detectable IgM-producing antigen-specific cells at these sites. Thus, both IgA CSR and SHM, as well as affinity maturation are two very prominent traits of IgA responses in the GALT.<sup>1-4</sup>

By conjugating NP to CT, we developed a tool to uncover the buildup of a specific TD-IgA response after oral immunization. Whereas earlier studies were limited to the detection of specific antibody production following oral priming immunization, we



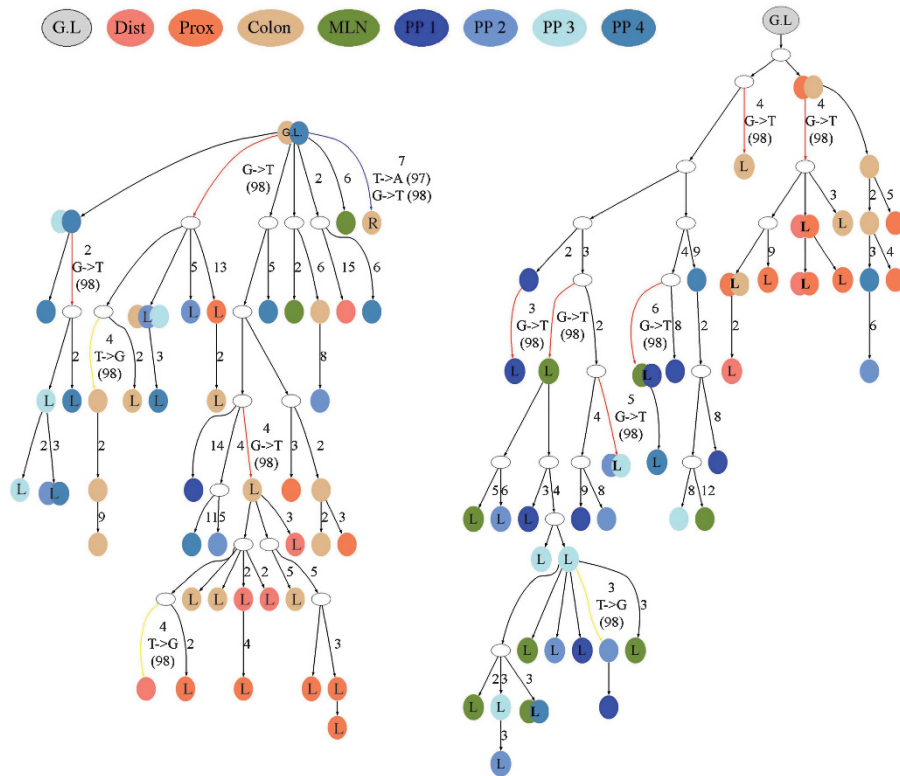
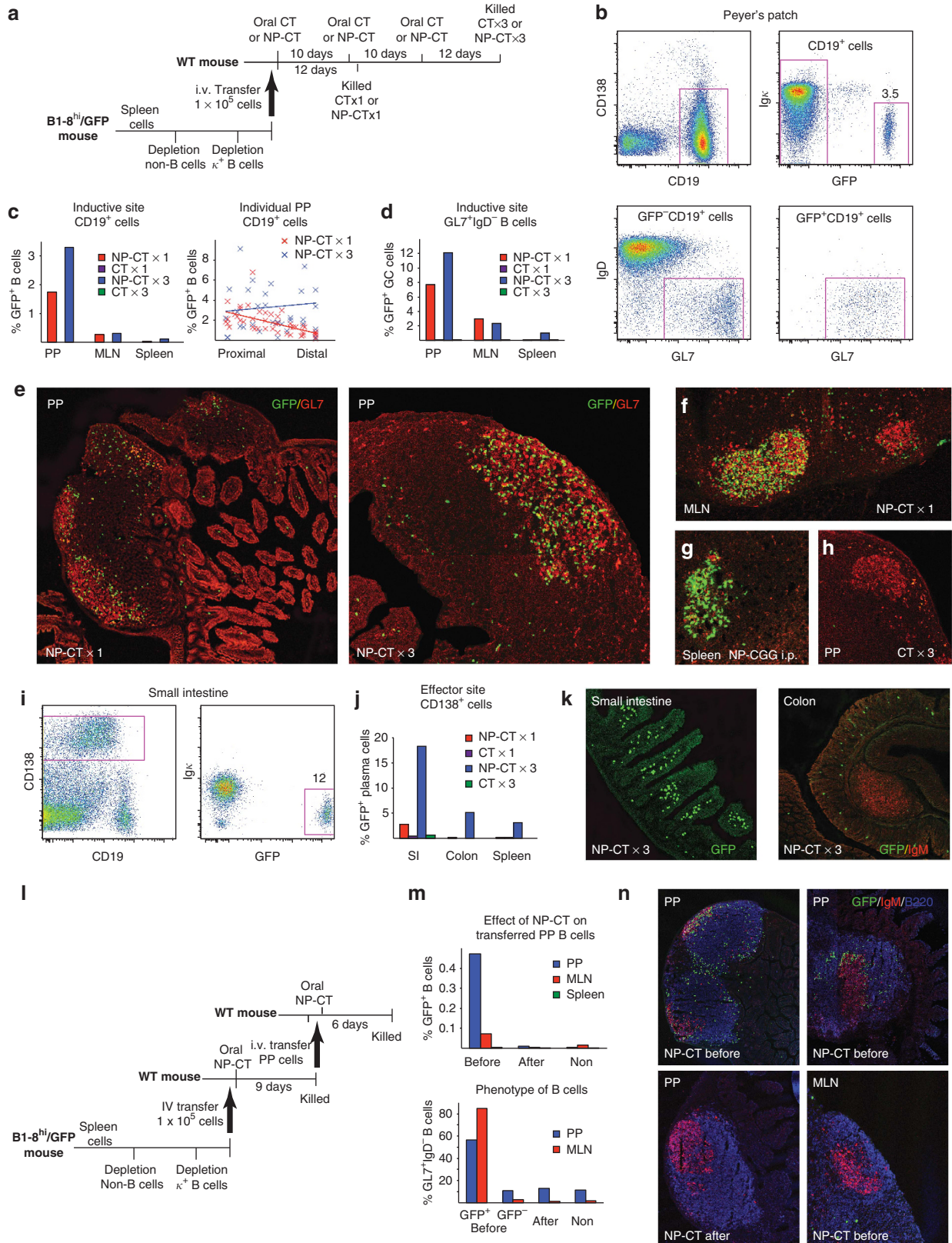


**Figure 7** Clonal tree analysis of antigen-specific IgA B-cell responses following oral immunization demonstrates extensive clonal relationships throughout the entire gut immune system. The *VH186.2-DFL 16.1* IgA sequences from four mice immunized three times orally with hapten (4-hydroxy-3-nitrophenyl)acetyl-cholera toxin (NP-CT) were analyzed for clonal relationships. Ig gene clones were transformed into mutational lineage trees using IgTree®,<sup>53</sup> implementing a distance method-based algorithm that finds the most likely tree with a high probability. Original sequences found in the experiments are assigned to either leaves or internal nodes of the tree. Each tree node represents a single mutation separating the sequences. The mutations that separate the sequences from each other can be point mutations, deletions or insertions, or gaps, which are considered single mutations. One to three clonal trees were identified from each mouse. Two of these trees, isolated from two different mice, are shown. Unique sequences were color-coded based on their tissue origin, and the numbers of mutations between each two successive nodes are denoted. Red lines indicate the location of the key mutation on the tree at position 33. Some of the lower branches contained sequences from several inductive and effector sites, suggesting an ongoing exchange of affinity-matured IgA B cells between these sites even late during the immune response.

**Figure 8** Hapten (4-hydroxy-3-nitrophenyl)acetyl (NP)-specific B cells invade pre-existing germinal centers (GCs) in Peyer's patches (PPs) after a single NP-cholera toxin (CT) immunization. **(a)** NP-specific splenic B cells were isolated from B1-8<sup>hi</sup> GFP mice<sup>46</sup> carrying a prearranged high-affinity NP-binding Ig heavy-chain gene through negative selection by magnetic bead depletion of non-B cells and κ light-chain B cells and transferred into the wild-type (WT) mice that were orally NP-CT immunized one or three times. **(b and c)** The proportion of GFP<sup>+</sup> CD19<sup>+</sup> B cells in individual PPs, MLNs, and spleen were determined using specific antibody labeling and flow cytometry. To the left in **(c)** is shown the proportion of GFP<sup>+</sup> CD19<sup>+</sup> B cells in the different tissues, and to the right the mean frequency of GFP<sup>+</sup> CD19<sup>+</sup> B cells in six to nine individual PPs ranging from proximal to distal location in the intestines of six mice. There was a statistically uneven distribution of GFP-expressing cells according to Kruskal–Wallis ( $P < 0.0001$ ) in **a**, with Dunn's post-test showing significant ( $P < 0.05$ ) differences between PPs compared to MLNs or spleen after both one and three immunizations. The linear regression between proximal and distal PP with regard to GFP<sup>+</sup> B-cell expansion was statistically significant different from zero after one ( $P < 0.0001$ ) but not three ( $P = 0.6558$ ) oral immunizations. **(d)** The proportion of GFP<sup>+</sup> cells among GL7<sup>+</sup> IgD<sup>-</sup> GC phenotype B cells in PPs, MLNs, and spleen was determined after one or three oral immunizations. There was statistically uneven distribution of GFP-expressing cells according to Kruskal–Wallis analysis ( $P < 0.0001$ ), with Dunn's post-test showing significant ( $P < 0.05$ ) differences between PPs compared to MLNs or spleen after both one and three oral immunizations. **(e–h)** Micrographs demonstrating the presence of GFP<sup>+</sup> cells (green) in GL7<sup>+</sup> (red) GCs. Overview pictures of PPs after one and three immunizations are shown in **(e)**. After oral immunization, GFP<sup>+</sup> B cells were never as tightly clustered in the PP as in the MLN or spleen after intraperitoneal (i.p.) priming with NP-CGG and alum. **(f and g)** Oral immunization with CT only did not attract any GFP<sup>+</sup> cells to the PP **(h)**. The proportions of GFP<sup>+</sup> CD138<sup>+</sup> plasma cells in the small intestine (SI), colon, and spleen were determined using flow cytometry after one or three oral immunizations with NP-CT or CT **(i and j)**. GFP<sup>+</sup> plasma cells were identified in the lamina propria of the SI and colon, but not in the isolated lymphoid follicle (ILF) **(k)**. To prove that GL7<sup>+</sup> PP B cells could migrate into already existing PP, we adoptively transferred such cells from mice 9 days after they were given a single oral NP-CT dose into recipient mice **(l)**. The latter mice were either untreated or given NP-CT 24 h before or after the transfer of PP cells. NP-primed GFP<sup>+</sup> donor PP B cells appeared in multiple PPs and to some extent in MLNs in the recipient mice given oral NP-CT 24 h before transfer **(m and n)**. In contrast, no GFP<sup>+</sup> PP B cells were found in the recipient PP in untreated mice or mice treated with NP-CT 24 h after the transfer. The majority of GFP<sup>+</sup> cells maintained a GL7<sup>+</sup> IgD<sup>-</sup> GC phenotype in both the PP and MLN, although they only entered the GC in the PP **(m and n)**. These are representative results of at least two experiments giving similar results. GFP, green fluorescent protein.

employed a more sensitive assay for early antigen-specific B-cell responses in the GALT by detecting NP-specific  $V_H186.2$ -IgA and -IgM gene usage.<sup>27,30,39</sup> We consistently found rare NP-specific  $V_H186.2$ -IgM sequences in the PP, but not in the MLN

or LP, indicating that PP was the first site for antigen activation of specific B cells. This result also corroborated the previous, less precise ELISPOT findings, showing that the IgA responses in the PP precede those in the MLN and LP.<sup>26-28</sup> This notion



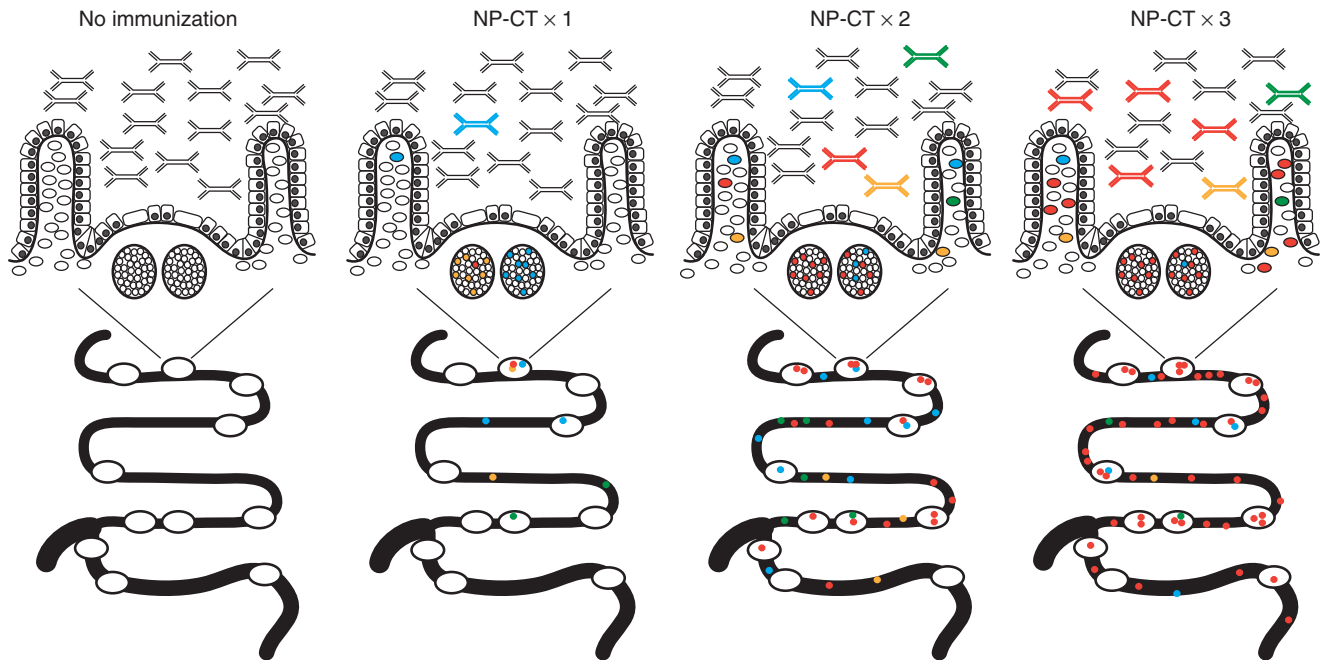


**Figure 9** A model for how synchronized, oligoclonal, and high-affinity gut IgA responses develop after oral immunization. Before immunization, very few hapten (4-hydroxy-3-nitrophenyl)acetyl (NP)-specific B cells exist in the gut-associated lymphoid tissue (GALT) or lamina propria (LP). However, early on after an oral priming immunization with NP-cholera toxin (CT)-responding B cells are expanded and distributed to multiple Peyer's patches (PPs), where they can undergo additional expansion and affinity maturation after the second and third oral immunization before migrating to the mesenteric lymph node (MLN), and subsequently being seeded into the LP of the small and large intestines. Whereas an oral priming will attract many antigen-specific B cells (orange, green, blue), occasionally a high-affinity clone (red) will be generated in a germinal center (GC) and distributed to pre-existing GCs in multiple PPs. Owing to affinity maturation, the high-affinity clone (red) will be selected and expanded in the GC by re-exposure to antigen and quickly dominate the response in multiple PPs. After a third immunization, predominantly high-affinity clones (red) have migrated to the gut LP, resulting in a synchronized production of high-affinity IgA antibodies.

was further strengthened by the strong expansion of NP-specific GFP<sup>+</sup> B cells in the PP and not in the MLN after a single oral immunization in our B1-8<sup>hi</sup> NP-specific IgH knock-in B-cell transfer model system.

Previous studies have clearly indicated that gut IgA B-cell responses against TD antigens largely emanate from the PP, rather than the MLN or ILF, although anti-bacterial IgA responses against, e.g., *Salmonella* may be stimulated in ILFs in the absence of the PP and MLN.<sup>24,40,41</sup> We found no evidence for the ILF being a site for initiation of a specific IgA response to a TD antigen following oral immunization. This observation also agrees well with previous studies, which have demonstrated that ILFs develop as a consequence of bacterial colonization and perturbed functions in the PP, such as deficiency in activation-induced cytidine deaminase, which will lead to hyperplasia of ILFs, as will intrauterine treatment with LTβR-Ig fusion protein to ablate PP development.<sup>24,42,43</sup> Hence, it is unlikely that ILFs are involved in generating IgA responses against TD antigens following oral immunizations, although they have been found to host significant IgA CSR, probably driven by bacterial antigens.<sup>17,38</sup>

In contrast, we found *V<sub>H</sub>186.2-IgA* gene expression in cPs, suggesting that these organized lymphoid tissues were indeed involved in TD-specific IgA responses. Apart from one study

of intrarectal immunization with ovalbumin admixed with CT adjuvant, little has been published on cPs and their role in gut IgA responses.<sup>9,40</sup> That study demonstrated that cP-depleted mice failed to respond with IgA antibodies following immunization, but whether the IgA B-cell response emanated from cPs was not directly investigated. One reason for the few publications on cPs may be that, contrary to PPs, they cannot be identified by macroscopic inspection and, therefore, only careful microscopic dissection of the tissue will allow the study of cPs. This restricts the analysis of specific B-cell responses, requiring microscopic analysis of labeled tissue sections. From this work, we could appreciate that each colon had 1–3 cPs, which were clearly well-organized secondary lymphoid structures. In the literature, they are described mostly in the context of inflammatory lesions and appear to be dependent on LTβR signaling, similar to PPs.<sup>44</sup> Gene sequence analysis revealed that the NP-specific *V<sub>H</sub>186.2-IgA* responses were clonally related to those observed in PPs, suggesting that cPs are an intricate part of the IgA inductive system in the GALT. Whether cPs and PPs perform different functions will be the focus of further studies.

Following oral immunization, we observed specific plasma cells along the entire small and large intestines. By sequencing *V<sub>H</sub>186.2-IgA* genes in many different tissues, organized

as well as non-organized, we could compile extensive trees of clonal relationships based on similarities in the CDR3 region. Importantly, we secured that our PCR method was sufficiently sensitive to detect  $V_H186.2$ -IgA genes in both PP B cells and LP plasma cells, and hence we could follow the buildup of a TD-dependent gut IgA response following oral immunization. Strikingly, we obtained patterns illustrating an exceptionally efficient distribution of clonally related high-affinity IgA cells to both the GALT and the LP. Even the colon and the cP carried NP-specific cells that were clonally related to those found in the PP, MLN and small intestinal LP. The gut IgA response required multiple doses. A single oral dose stimulated barely detectable NP-specific IgA cells in the LP and only a few in MLN, whereas antigen-specific B cells significantly expanded in the PP. Most of the NP-specific B cells had undergone IgA CSR and few remained IgM B cells in the PP after a single dose, indicating that IgA CSR occurred at an early stage of the response, before SHM and affinity maturation. This agrees well with our previous findings of IgA CSR in the PP of CD40-deficient mice and that many IgA<sup>+</sup> B cells in the PP express activation-induced cytidine deaminase and have a GC phenotype.<sup>17,45</sup>

Our results showing that 60–70% of the canonical  $V_H186.2$ -IgA NP-binding cells after three oral immunizations were high-affinity cells with the characteristic mutation in the CDR1 region,  $W_{33} \Rightarrow L_{33}$ , in both the PP and LP agrees well with the classical studies by Cumano and Rajewsky<sup>46</sup> demonstrating similar frequencies of this mutation in secondary-type splenic responses. This result argues for a strong selection process of activated B cells in the GALT. As this high frequency was reached in the PP IgA B cells after two oral immunizations and only after three oral immunizations in plasma cells in the LP, this logically speaks in favor of the PP being the site of initiation of the gut IgA response to TD antigens. Additional evidence in support of this interpretation were the facts that oral immunization primarily induced GL7<sup>+</sup> GFP<sup>+</sup> B cells in the PP using a B1-8<sup>hi</sup> NP-specific IgH knock-in B-cell transfer model and that the PP was the only tissue to carry NP-specific  $V_H186.2$ -IgM gene sequences following oral immunizations. Previous studies have shown that  $\lambda 1$ -chain bearing  $V_H186.2$ -DFL16.1 NP-specific B cells greatly dominated the response in the spleen after systemic immunizations with NP-chicken  $\gamma$ -globulin.<sup>33</sup> These gene sequences were generally heavily mutated, whereas non-canonical genes or related genes were unmutated. After repeated oral immunizations, we found that canonical  $V_H186.2$ -IgA genes in both PP and LP were heavily mutated, supporting that in this regard the gut NP-specific response resembled that observed following systemic immunizations.

The picture that emerges from these studies of gut IgA responses to TD antigens is strikingly different from that reported for IgA responses to the commensal flora.<sup>47</sup> While IgA responses to the commensal flora appear multi-centered and diverse, as documented by earlier studies showing IgA responses in the GALT, including the ILFs, and MLNs as well as the LP itself,<sup>12,47,48</sup> the IgA response to NP-CT was initiated and synchronized in PP, and strongly oligoclonal and dominated by high-affinity IgA plasma cells along the entire small and large

intestines. Thus, this broad distribution of antigen-specific high-quality IgA cells clearly provides strong functionality and allows for the development of protective immunity against pathogens in the gut mucosa, irrespective of where an infection is located. Multiple oral immunizations were required for a strong IgA response in the LP. The reason for this, we believe, is the requirement for antigen-driven expansion of high-affinity IgA B cells being distributed to and expanded in the GC in multiple PPs, and perhaps involving cPs and MLNs as well. On the basis of the clonal relationships between NP-specific IgA cells in multiple PPs and the findings using the GFP<sup>+</sup> NP-specific B-cell transfer model in this study, we concluded that the effectiveness of this system rests on the re-utilization of already existing GC in the PPs. We found substantial expansion of GL7<sup>+</sup> GFP<sup>+</sup> NP-specific donor B cells in multiple PPs of recipient mice, provided oral NP-CT was given before transfer. Hence, upon repeated antigen challenge high-affinity IgA B-cell clones distributed to the GC in multiple PPs can be further expanded and matured before seeding the LP of the large and small intestines. This notion is indirectly supported by data from mucosal addressin, cell-adhesion molecule-1 (MadCam-1), deficient mice, which exhibited reduced gut IgA responses secondary to poor migration of B cells to the PP.<sup>49</sup> Such a dynamic function for GC in peripheral lymph nodes has, in fact, recently been described by Schwickert *et al.*<sup>50,51</sup> Our data, however, additionally suggest that not only naïve cells, but also cells with a GC phenotype can enter into pre-existing GCs if antigen is present. Given this information, it is understandable that oral vaccination using non-living antigens cannot be effective unless multiple doses are given. The gut IgA system simply requires multiple exposures to the antigen to select and expand high-affinity B-cell clones. This knowledge should be taken into consideration when future protocols for oral vaccination are designed.

## METHODS

**Mice and immunizations.** C57BL/6 and B1-8<sup>hi</sup> GFP<sup>+</sup>50 (generously provided by M Nussenzweig, Rockefeller University, New York, NY) mice were bred and housed at the animal facility Experimental Biomedicine (EBM) at the University of Gothenburg under specific pathogen-free conditions. Mice aged 6–10 weeks were used in the experiments. They were immunized with 20  $\mu$ g of NP-CT or 10  $\mu$ g CT alone as indicated. Repeated oral immunizations were performed 10 days apart, and mice were killed 8 days after the final immunization. Ethical approval for all experiments had been obtained.

**NP-CT conjugation.** CT was dialyzed in distilled water for 2 days before mixing it with an equal volume of 0.1 M NaHCO<sub>3</sub> and 20 equivalents NP-OSu (Biosearch Technologies, Novato, CA) per mole CT. The mixture was incubated for 12 h at 4 °C and transferred into a Slide-A-Lyzer dialysis cassette and dialyzed against 0.05 M NaHCO<sub>3</sub>, followed by water before the protein concentration was determined using a BCA assay (Thermo Fisher Scientific, Rockford, IL). The quality of conjugates was determined as described (**Supplementary Figure S1** online).

**Immunohistochemistry.** The mice were killed and the intestine, PP and MLN were embedded in TissueTek OCT compound and snap frozen in liquid nitrogen. Tissue containing GFP<sup>+</sup> cells were fixed in 4% paraformaldehyde and 10% sucrose for 1 h before freezing the tissue. Frozen sections (7  $\mu$ m) were fixed in 100% acetone and blocked with normal horse serum in phosphate-buffered saline (PBS) (5%) for 15 min. The

sections were stained for 1 h with optimal concentrations of biotin-conjugated anti-GL7 mAb (eBioscience, San Diego, CA), followed by AlexaFlour594-streptavidin (Life Technologies, Carlsbad, CA), Texas red- or FITC-conjugated anti-IgM (Southern Biotech, Birmingham, AL), FITC-conjugated anti-IgA, FITC-conjugated B220 (BD Biosciences, San Jose, CA) and NP-PE (Biosearch Technologies). The sections were analyzed using the LSM 510 META confocal microscope (Carl Zeiss, Oberkochen, Germany).

**ELISPOT.** Ninety-six-well plates (Merck Millipore, Billerica, MA) were coated with  $5 \mu\text{g ml}^{-1}$  purified rat anti-mouse IgA antibodies (BD),  $3 \text{ nmol ml}^{-1}$  GM1-ganglioside followed by  $3 \mu\text{g ml}^{-1}$  CT or  $10 \mu\text{g ml}^{-1}$  NP-bovine serum albumin (BSA) (Biosearch Technologies) in PBS at  $4^\circ\text{C}$  overnight. The plates were washed in PBS, blocked with 0.2% BSA in PBS and  $10^5$  purified LP lymphocytes were added in duplicates and diluted 1:3 in four serial dilutions and incubated at  $37^\circ\text{C}$  for 3 h.<sup>52</sup> Specific antibodies were used to detect antibody-secreting cells; AP-conjugated goat anti-mouse IgA antibodies (Southern Biotech) were added and incubated overnight at  $4^\circ\text{C}$ . The AFC were visualized using BCIP substrate (Sigma-Aldrich, St Louis, MO) and analyzed using an Immunospot ELISPOT system (Cellular Technology Ltd, Shaker Heights, OH).

**ELISA.** Ninety-six-well plates (Thermo Fisher Scientific) were coated with  $100 \mu\text{l}$  per well of  $10 \mu\text{g ml}^{-1}$  NP-BSA,  $0.5 \text{ nM ml}^{-1}$  GM1 followed by  $0.5 \mu\text{g ml}^{-1}$  CT overnight at  $4^\circ\text{C}$ . The plates were treated as for ELISPOT before serum samples diluted 1:100 or gut lavages diluted 1:10 were added and a three- or twofold serial dilution was made, respectively. Samples were incubated overnight at  $4^\circ\text{C}$ , followed by isotype-specific AP-conjugated rat anti-mouse antibodies (Southern Biotech) at a dilution of 1:1,000 in PBS/0.1% BSA. The plates were developed using NPP substrate (Sigma) and analyzed at 405 nm using a Titertek Multiscan (MTX LabSystems, Vienna, VA) spectrophotometer.

**Flow cytometry and cell sorting.** Lymphocytes were isolated as described<sup>52</sup> and stained with PE-conjugated anti-CD138, PerCP-Cy5.5 anti-IgD, PECy7-conjugated anti-CD19, Alexa700-conjugated anti-Igk, anti-CD80 APC, and biotin-conjugated GL7 (BD), followed by Qdot605-conjugated streptavidin (Invitrogen) on ice. The cells were washed twice with FACS buffer and sorted or analyzed using a FACSAria or an LSR II (BD), respectively. Cells were sorted into tubes that had been coated with PBS with 2% BSA overnight and were pelleted by centrifugation at 600 g before being resuspended in PBS.

**RNA isolation, PCR, and Southern blot.** FACS-sorted PP CD80<sup>+</sup> CD138<sup>-</sup> B cells or whole PP or MLN tissue, microdissected tissue, or 1 cm pieces of the colon or small intestine were prepared and submerged in 350  $\mu\text{l}$  buffer RLT (Qiagen, Hilden, Germany). The tissue was disrupted and homogenized and RNA extracted using RNeasy minikits (Qiagen). cDNA synthesis was performed using an IgA- (5'-TGACATTGGTGGGTTTAC-3') or IgM- (5'-GAGGAAGAGGACGATGAA-3') specific primer and Superscript III RT polymerase (Invitrogen) at  $50^\circ\text{C}$  for 1 h. PCR primers were: IgA control PCR, IgA for (5'-CTGATACACGCAACACGCTT-3'), IgA down (5'-ACTCTAACCGCCGTCCAAGAA-3'); IgM control PCR, IgM up (5'-TGAATGTGTACACCTGCCGT-3'), IgM down (5'-GCTGACTCCCTCAGGTTTACG-3'); IgA NP PCR, IgA down2, (5'-TTCTCGAGGGATGGCAGGAAGGAGGAC-3'), NP leader up (5'-TCTAGAATTCGGGATGGAGCTGTATCATGCTC-3'); and IgM down PCR, IgM down2 (5'-TTCTCGAGAGGGCCAGAGAAGCCA TCC-3'), NP leader up (5'-TCTAGAATTCGGGATGGAGCTGTATCATGCTC-3'). All PCRs were carried out with an annealing temperature of  $64^\circ\text{C}$  using standard PCR protocols with 25 (IgA and IgM controls) or (NP-IgA or NP-IgM) 30 cycles. Products were separated by agarose gel electrophoresis and detected by Southern blotting with an NP probe (5'-CCGTAGTAATATCTTGACA-3') end-labeled with <sup>32</sup>P after transfer to a Hybond<sup>+</sup> membrane (GE Healthcare, Piscataway, NJ). Hybridization to the membrane was detected on a <sup>32</sup>P-sensitive phos-

phorus screen and analyzed using the PharosFX plus system (Bio-Rad, Hercules, CA).

**Cloning and sequencing.** PCR reactions for the cloning was performed as described above, but using the high-fidelity Phusion enzyme (Thermo Fisher Scientific). Samples were collected from two well-separated locations in the proximal and distal part of the small intestine, the colon, the MLN, and the PP. The PCR reactions were cloned into ZeroBlunt TOPO vectors (Invitrogen), transformed into bacteria, and single colonies were identified by colony hybridization using the NP probe. Plasmid minipreps were prepared using GeneElute kits (Sigma) from overnight cultures. Sequenced clones (Eurofins MWG Operon, Ebersberg, Germany) were analyzed using the Staden package. Clones were classified as NP binding if their CDR3 region was between 9 and 11 amino acids long, they had a tyrosine at position 99, and there were at least two more tyrosine residues in the following three amino acids.

**Lineage tree generation.** Lineage trees were generated using IgTree.<sup>53</sup>

**SUPPLEMENTARY MATERIAL** is linked to the online version of the paper at <http://www.nature.com/mi>

#### ACKNOWLEDGMENTS

This study was supported by the Swedish Research Council, the Swedish Cancer Foundation, the Sahlgrenska University Hospital LUA/ALF grants, The Norwegian Research Council Globvac program, Israel Science Foundation 270/09, Human Frontiers Science Program Research Grant, and MIVAC Swedish Foundation for Strategic Research. We acknowledge the Centre for Cellular Imaging at the University of Gothenburg for skilled support and Michel C. Nussenzweig for generously providing the B1-8<sup>high</sup> GFP mice. Finally, we would like to thank Dr Strober, NIH, for carefully reading the text and for helpful comments about the results and conclusions.

#### DISCLOSURE

The authors declared no conflict of interest.

© 2013 Society for Mucosal Immunology

#### REFERENCES

1. Strober, W., Fagarasan, S. & Lycke, N. IgA B cell development. In *Mucosal Immunology* 3rd edn (Mestecky, J., Lamm, M.E., Strober, W., Bienenstock, J., McGhee, J.R. & Mayer L, eds) 583–616 (Academic Press, Boston, MA, 2005).
2. Spencer, J., Barone, F. & Dunn-Walters, D. Generation of immunoglobulin diversity in human gut-associated lymphoid tissue. *Semin. Immunol.* **21**, 139–146 (2009).
3. Brandtzaeg, P. Update on mucosal immunoglobulin A in gastrointestinal disease. *Curr. Opin. Gastroenterol.* **26**, 554–563 (2010).
4. Macpherson, A.J., McCoy, K.D., Johansen, F.E. & Brandtzaeg, P. The immune geography of IgA induction and function. *Mucosal Immunol.* **1**, 11–22 (2008).
5. Fagarasan, S., Kawamoto, S., Kanagawa, O. & Suzuki, K. Adaptive immune regulation in the gut: T cell-dependent and T cell-independent IgA synthesis. *Annu. Rev. Immunol.* **28**, 243–273 (2010).
6. Brandtzaeg, P. Induction of secretory immunity and memory at mucosal surfaces. *Vaccine* **25**, 5467–5484 (2007).
7. Macpherson, A.J. IgA adaptation to the presence of commensal bacteria in the intestine. *Curr. Top. Microbiol. Immunol.* **308**, 117–136 (2008).
8. McDonald, K.G., McDonough, J.S. & Newberry, R.D. Adaptive immune responses are dispensable for isolated lymphoid follicle formation: antigen-naïve, lymphotoxin-sufficient B lymphocytes drive the formation of mature isolated lymphoid follicles. *J. Immunol.* **174**, 5720–5728 (2005).
9. Lee, A.Y. *et al.* Dendritic cells in colonic patches and iliac lymph nodes are essential in mucosal IgA induction following intrarectal administration via CCR7 interaction. *Eur. J. Immunol.* **38**, 1127–1137 (2008).
10. Fagarasan, S., Kinoshita, K., Muramatsu, M., Ikuta, K. & Honjo, T. *In situ* class switching and differentiation to IgA-producing cells in the gut lamina propria. *Nature* **413**, 639–643 (2001).

11. Uematsu, S. *et al.* Regulation of humoral and cellular gut immunity by lamina propria dendritic cells expressing Toll-like receptor 5. *Nat. Immunol.* **9**, 769–776 (2008).
12. Tsuji, M. *et al.* Requirement for lymphoid tissue-inducer cells in isolated follicle formation and T cell-independent immunoglobulin a generation in the gut. *Immunity* **29**, 261–271 (2008).
13. Bemark, M., Boysen, P. & Lycke, N.Y. Induction of gut IgA production through T cell-dependent and T cell-independent pathways. *Ann. N.Y. Acad. Sci.* **1247**, 97–116 (2012).
14. Craig, S.W. & Cebra, J.J. Peyer's patches: an enriched source of precursors for IgA-producing immunocytes in the rabbit. *J. Exp. Med.* **134**, 188–200 (1971).
15. Husband, A.J. & Gowans, J.L. The origin and antigen-dependent distribution of IgA-containing cells in the intestine. *J. Exp. Med.* **148**, 1146–1160 (1978).
16. Bergqvist, P., Gärdby, E., Stensson, A., Bemark, M. & Lycke, N.Y. Gut IgA class switch recombination in the absence of CD40 does not occur in the lamina propria and is independent of germinal centers. *J. Immunol.* **177**, 7772–7783 (2006).
17. Bergqvist, P., Stensson, A., Lycke, N.Y. & Bemark, M. T cell-independent IgA class switch recombination is restricted to the GALT and occurs prior to manifest germinal center formation. *J. Immunol.* **184**, 3545–3553 (2010).
18. Wei, M., Shinkura, R., Doi, Y., Maruya, M., Fagarasan, S. & Honjo, T. Mice carrying a knock-in mutation of Aicda resulting in a defect in somatic hypermutation have impaired gut homeostasis and compromised mucosal defense. *Nat. Immunol.* **12**, 264–270 (2011).
19. Griebel, P.J. & Hein, W.R. Expanding the role of Peyer's patches in B-cell ontogeny. *Immunol. Today* **17**, 30–39 (1996).
20. Yamamoto, M. *et al.* Alternate mucosal immune system: organized Peyer's patches are not required for IgA responses in the gastrointestinal tract. *J. Immunol.* **164**, 5184–5191 (2000).
21. Macpherson, A.J. & Uhr, T. Induction of protective IgA by intestinal dendritic cells carrying commensal bacteria. *Science* **303**, 1662–1665 (2004).
22. Tezuka, H. *et al.* Prominent role for plasmacytoid dendritic cells in mucosal T cell-independent IgA induction. *Immunity* **34**, 247–257 (2011).
23. Lorenz, R.G. & Newberry, R.D. Isolated lymphoid follicles can function as sites for induction of mucosal immune responses. *Ann. N.Y. Acad. Sci.* **1029**, 44–57 (2004).
24. Yamamoto, M. *et al.* Role of gut-associated lymphoreticular tissues in antigen-specific intestinal IgA immunity. *J. Immunol.* **173**, 762–769 (2004).
25. Hörnquist, E. & Lycke, N. Cholera toxin adjuvant greatly promotes antigen priming of T cells. *Eur. J. Immunol.* **23**, 2136–2143 (1993).
26. Lycke, N. The mechanism of cholera toxin adjuvanticity. *Res. Immunol.* **148**, 504–520 (1997).
27. Hahn, A., Thiessen, N., Pabst, R., Buettner, M. & Bode, U. Mesenteric lymph nodes are not required for an intestinal immunoglobulin A response to oral cholera toxin. *Immunology* **129**, 427–436 (2010).
28. Gärdby, E., Wrammert, J., Schön, K., Ekman, L., Leanderson, T. & Lycke, N. Strong differential regulation of serum and mucosal IgA responses as revealed in CD28-deficient mice using cholera toxin adjuvant. *J. Immunol.* **170**, 55–63 (2003).
29. Allen, D., Simon, T., Sablitzky, F., Rajewsky, K. & Cumano, A. Antibody engineering for the analysis of affinity maturation of an anti-hapten response. *EMBO J.* **7**, 1995–2001 (1988).
30. Takahashi, Y., Dutta, P.R., Cerasoli, D.M. & Kelsoe, G. *In situ* studies of the primary immune response to (4-hydroxy-3-nitrophenyl)acetyl. V. Affinity maturation develops in two stages of clonal selection. *J. Exp. Med.* **187**, 885–895 (1998).
31. Jacob, J., Przylepa, J., Miller, C. & Kelsoe, G. *In situ* studies of the primary immune response to (4-hydroxy-3-nitrophenyl)acetyl. III. The kinetics of V region mutation and selection in germinal center B cells. *J. Exp. Med.* **178**, 1293–1307 (1993).
32. Holmgren, J., Lönnroth, I., Månsson, J. & Svennerholm, L. Interaction of cholera toxin and membrane GM1 ganglioside of small intestine. *Proc. Natl. Acad. Sci. USA* **72**, 2520–2524 (1975).
33. Weiss, U. & Rajewsky, K. The repertoire of somatic antibody mutants accumulating in the memory compartment after primary immunization is restricted through affinity maturation and mirrors that expressed in the secondary response. *J. Exp. Med.* **172**, 1681–1689 (1990).
34. Anderson, S.M., Tomayko, M.M., Ahuja, A., Haberman, A.M. & Shlomchik, M.J. New markers for murine memory B cells that define mutated and unmutated subsets. *J. Exp. Med.* **204**, 2103–2114 (2007).
35. Bemark, M., Bergqvist, P., Stensson, A., Holmberg, A., Mattsson, J. & Lycke, N.Y. A unique role of the cholera toxin A1-DD adjuvant for long-term plasma and memory B cell development. *J. Immunol.* **186**, 1399–1410 (2011).
36. Tabibian-Keissar, H. *et al.* B-cell clonal diversification and gut-lymph node trafficking in ulcerative colitis revealed using lineage tree analysis. *Eur. J. Immunol.* **38**, 2600–2609 (2008).
37. Barone, F. *et al.* IgA-producing plasma cells originate from germinal centers that are induced by B-cell receptor engagement in humans. *Gastroenterology* **140**, 947–956 (2011).
38. Shikina, T. *et al.* IgA class switch occurs in the organized nasopharynx- and gut-associated lymphoid tissue, but not in the diffuse lamina propria of airways and gut. *J. Immunol.* **172**, 6259–6264 (2004).
39. Lycke, N. & Holmgren, J. Strong adjuvant properties of cholera toxin on gut mucosal immune responses to orally presented antigens. *Immunology* **59**, 301–308 (1986).
40. Newberry, R.D. & Lorenz, R.G. Organizing a mucosal defense. *Immunol. Rev.* **206**, 6–21 (2005).
41. Martinoli, C., Chiavelli, A. & Rescigno, M. Entry route of *Salmonella typhimurium* directs the type of induced immune response. *Immunity* **27**, 975–984 (2007).
42. Fagarasan, S., Muramatsu, M., Suzuki, K., Nagaoka, H., Hiai, H. & Honjo, T. Critical roles of activation-induced cytidine deaminase in the homeostasis of gut flora. *Science* **298**, 1424–1427 (2002).
43. Lorenz, R.G., Chaplin, D.D., McDonald, K.G., McDonough, J.S. & Newberry, R.D. Isolated lymphoid follicle formation is inducible and dependent upon lymphotoxin-sufficient B lymphocytes, lymphotoxin beta receptor, and TNF receptor I function. *J. Immunol.* **170**, 5475–5482 (2003).
44. Dohi, T. *et al.* Elimination of colonic patches with lymphotoxin beta receptor-Ig prevents Th2 cell-type colitis. *J. Immunol.* **167**, 2781–2790 (2001).
45. Crouch, E.E. *et al.* Regulation of AID expression in the immune response. *J. Exp. Med.* **204**, 1145–1156 (2007).
46. Cumano, A. & Rajewsky, K. Clonal recruitment and somatic mutation in the generation of immunological memory to the hapten NP. *EMBO J.* **5**, 2459–2468 (1986).
47. Hapfelmeier, S. *et al.* Reversible microbial colonization of germ-free mice reveals the dynamics of IgA immune responses. *Science* **328**, 1705–1709 (2010).
48. He, B. *et al.* Intestinal bacteria trigger T cell-independent immunoglobulin A2 class switching by inducing epithelial-cell secretion of the cytokine APRIL. *Immunity* **26**, 812–826 (2007).
49. Schippers, A. *et al.* Mucosal addressin cell-adhesion molecule-1 controls plasma-cell migration and function in the small intestine of mice. *Gastroenterology* **137**, 924–933 (2009).
50. Schwickert, T.A. *et al.* *In vivo* imaging of germinal centres reveals a dynamic open structure. *Nature* **446**, 83–87 (2007).
51. Schwickert, T.A., Alabyev, B., Manser, T. & Nussenzweig, M.C. Germinal center reutilization by newly activated B cells. *J. Exp. Med.* **206**, 2907–2914 (2009).
52. Lefrançois, L. & Lycke, N. Isolation of mouse small intestinal intraepithelial lymphocytes, Peyer's patch, and lamina propria cells. *Curr. Protoc. Immunol.* (Chapter 3: Unit 3.19.1–3.19.16) (2001).
53. Barak, M., Zuckerman, N.S., Edelman, H., Unger, R. & Mehr, R. IgTree: creating immunoglobulin variable region gene lineage trees. *J. Immunol. Methods* **338**, 67–74 (2008).